Doubling throughput in urban roads by platooning ⋆

Jennie Lioris * **Ramtin Pedarsani** ** **Fatma Yildiz Tascikaraoglu** *** **Pravin Varaiya** ****

* *Ecole des Ponts ParisTech, ENPC, France, (e-mail: jennie.lioris@cermics.enpc.fr)*
** *Department of Electrical Engineering and Computer Sciences, University of California, Berkeley, CA, U.S.A., (e-mail: ramtin@berkeley.edu)*
*** *Department of Control and Automation Engineering, Istanbul, Turkey, (e-mail: fayildiz@yildiz.edu.tr)*
**** *Department of Electrical Engineering and Computer Sciences, University of California, Berkeley, CA, U.S.A., (e-mail: varaiya@berkeley.edu)*

Abstract: Intersections are the bottlenecks of the urban road system because an intersection's capacity is only a fraction of the vehicle flows that the roads connecting to the intersection can carry. The saturation flow rate, and hence the capacity, can be doubled if vehicles can cross intersections in platoons rather than one by one as they do today. Platoon formation is enabled by connected vehicle technology. Doubling the saturation flow rate has dramatic mobility benefits: the throughput of the road system can be doubled without changing the signal control, or vehicle delay can be reduced by reducing the cycle time. These predictions draw on an analysis of a queuing model of a signalized network with fixed time control and they are validated in a simulation of a small urban network with 16 intersections and 73 links.

Keywords: Five to ten keywords, preferably chosen from the IFAC keyword list.

1 Introduction

Connected vehicle technology (CVT) is founded on the capability of vehicles to communicate in a mobile environment using dedicated short-range communications (DSRC). CVT has aroused interest in the academic community and in automobile and IT companies.

Academic research has shown that DSRC can support mobile networks with vehicle-to-vehicle (V2V) and vehicle-to-infrastructure (V2I) communication (Bezzina and Sayer (2015)). There also is research on coordinated vehicle control using V2V communication to enable maneuvers such as merging, cooperative adaptive cruise control (CACC) (Ploeg et al. (2011); Kianfar et al. (2012); Milanes et al. (2014)) and passage through an intersection without signals (Au et al. (2015)). The NHTSA report (Harding et al. (2014)) describes the enhanced safety that V2V communications potentially offers in pre-crash scenarios. Commercial effort in CVT seeks to stimulate and meet consumer demand to connect cars to the internet. None of this research is concerned with enhancing mobility.

By contrast, this paper explores the use of CVT to dramatically increase the capacity of urban roads based on the simple idea that if CVT can enable organizing vehicles into platoons, the capacity of an intersection can be increased by a factor of two to three. §2 sketches a scenario showing how platooning increases an intersection's capacity by increasing its saturation flow rate. It points to research that demonstrates platooning using cooperative adaptive cruise control (CACC) implemented on ACC-equipped commercial vehicles augmented with V2V communication. §3 analyzes a queuing network model to show that an increase in the saturation flow rate by a factor γ can support an increase in demand in the same proportion, with no change in the signal control. Alternatively, the gain γ can be used to reduce the intersection delay by reducing the cycle time, while maintaining the red clearance times. The simulation exercise in §4 confirms these predictions. §6 summarizes the main conclusions of this study.

⋆ This research was supported by the California Department of Transportation and TUBITAK-2219 program. We thank Rene Sanchez of Sensys Networks for the data in Figure 1, and Alex A. Kurzhanskiy, Gabriel Gomes, Roberto Horowitz and Sam Coogan and others in the Berkeley Friday Arterial seminar for stimulating discussions.

2 Intersection capacity

The Highway Capacity Manual (HCM) defines an intersection's capacity as

$$\text{Capacity} = \sum_i s_i \frac{g_i}{T}. \tag{1}$$

Here T is the cycle time and, for lane group i, s_i is the saturation flow rate and g_i/T is the effective green ratio. HCM takes $s_i = N \times s_0 \times f$: N is the number of lanes in the group, s_0 is the base rate in vehicles per hour (vph), and f is an 'adjustment factor' that depends on the road geometry and traffic characteristics. HCM suggests $s_0 = 1,900$ vph. Since $s_i \times (g_i/T)$ is the rate at which vehicles in queue in group i can potentially be served by the intersection, we also call it the *service rate* in a queuing model of this lane group.

Consider an intersection with four approaches, each with one through lane and one left-turn lane. There are thus eight movements in all, two movements per approach. If each lane supports a flow of 1,900 vph, the four approaches can carry a total of

Number	Time after phase starts	Time before phase ends	Occupancy sec	Speed mph
1	3.47	47.28	63.88	17.53
2	5.85	44.91	0.44	28.33
3	8.35	42.41	0.81	33.43
4	11.22	39.53	0.81	24.52
5	14.16	36.59	0.56	33.53
6	25.53	25.22	0.31	52.75
7	33.41	17.34	0.44	52.75
8	34.1	16.66	0.38	52.51
9	36.41	14.34	0.56	40.93
10	37.91	12.84	0.56	52.75
11	39.1	11.65	0.5	40.93
12	45.03	5.72	0.12	73.72

Fig. 1. A trace of vehicles entering an intersection from one through lane during one green phase.

$1,900 \times 8 = 15,200$ vph. However, only two movements can safely be permitted at the same time, so the effective green ratio for each movement is at most 0.25, and from equation (1) the capacity of the intersection is only 3,800 vph. Thus the intersection is the principal bottleneck in urban roads: its capacity is a fraction (here 1/4) of the capacity of the roads connecting to it.

Figure 1 displays the measured trace of detector events from 12 vehicles that enter a through lane in an intersection during one cycle with a green phase duration of 50 sec for the through movement. The second and third columns give the times (in sec) after the start of green and before the end of green when each vehicle enters the intersection, the fourth column gives the duration of time the vehicle 'occupied' the detector zone, and the fifth column lists an estimate of its speed. The detectors have a sampling frequency of 16 Hz, so the speeds are quantized: speeds above 60 mph have a quantization error of about 15 mph, speeds below 30 mph have an error under 5 mph. The average speed of the 12 vehicles is 42 mph. The speed limit at this intersection is 50 mph. The first vehicle entering the intersection has a delay or reaction time of 3.47 sec. The first 5 vehicles enter within 14.16 sec, so the empirical saturation flow rate of this movement is 14.16/5 = 2.83 sec per veh or 3600/2.83 = 1272 veh/hour. Vehicles 5, 6, $\cdots$ travel at much higher speed. Note that the time headway between vehicles 7 and 8 is only 0.7 sec.

Suppose these 12 vehicles were to move together as a platoon at a speed of 45 mph (66 feet/sec) and a uniformly small time headway of (say) 0.75 s. This would give a saturation flow rate of $3600/0.75 = 4800$ vph, which is 3.8 times the observed rate of 1272 vph and 2.5 times HCM's theoretical rate of 1900 vph. A quick estimate for a platoon crossing an intersection at 30 mph (44 feet/sec) with space headway of 40 feet (time headway of 40/44 s) is a platoon saturation flow rate of (44/40) $\times$ 3600 = 3960 vph, which is twice HCM's 1900 vph and up to three times the rates observed in today's intersections.

What does it take to organize a platoon? If the 12 vehicles queued at or approaching the intersection were 'connected' that is, if they were to communicate with each other as well as with the signal controller, their longitudinal motion could be coordinated in such a way that they would move together as a platoon and thereby increase the saturation flow rate by a factor of two or three. Milanes et al. (2014) report an experiment of a 4-vehicle platoon, capable of cut-in, cut-out and other maneuvers, using CACC technology. The vehicles had factory-equipped ACC and their capability was enhanced by a DSRC radio that permitted V2V communication needed to enable CACC. The vehicles in the platoon experiment had a time gap of 0.6 sec (time headway of 0.8 s) traveling at 55 mph. Ploeg et al. (2011) report an experiment of a 6-vehicle CACC platoon, with a 0.5s headway. The ACC equipped vehicles were augmented with V2V communications using a 802.11a WiFi radio in ad-hoc mode.

It is important to distinguish our proposal to use CACC to increase an intersection's capacity from proposals to use CACC to increase a highway's capacity by decreasing headway. Increasing the throughput of urban roads will *not* increase the throughput of the urban network which is limited by intersection capacity.

3 Three predictions

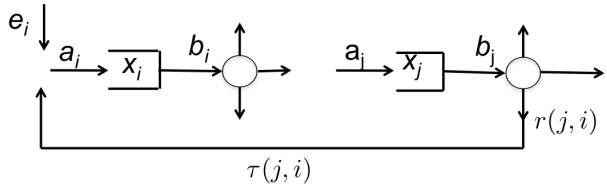

Fig. 2. Fluid network model. Source: Muralidharan et al. (2015).

Imagine that all saturation flow rates in an urban road network of signalized intersections are increased by the same factor of 2 to 3 using platoons. We explore the implications of such a productivity increase, assuming that all signals use a fixed-time control with the same cycle time T. We use a fluid model of a network of signalized intersections for our exploration. The model is studied by Muralidharan et al. (2015) and illustrated in Figure 2.

There are J queues in the network, each corresponding to one turn movement. A specified fraction $r(j,i)$ of the vehicles departing from queue j is routed to queue i. Queue i also has exogenous arrivals with rate $e_i(t)$. The exogenously specified service rate of queue i, $c_i(t)$, is periodic with period T: $c_i(t)$ is the saturation flow rate when the light is green and $c_i(t) = 0$, when it is red. $x_i(t)$ is the queue length of i and $b_i(t)$ is its departure rate at time t. $a_i(t)$ denotes the total arrival rate into queue i at time t. The travel time from queue j to queue i on link (j,i) is $\tau(j,i)$ as in the figure. The network dynamics are as follows.

$$\dot{x}_i(t) = a_i(t) - b_i(t), \tag{2}$$

$$a_i(t) = e_i(t) + \sum_{j=1}^{J} b_j(t - \tau(j,i)) r(j,i), \tag{3}$$

$$b_i(t) = \begin{cases} c_i(t), & \text{if } x_i(t) > 0, \\ \in [0, c_i(t)], & \text{if } x_i(t) = 0, \\ 0, & \text{if } x_i(t) < 0. \end{cases} \tag{4}$$

(2) says that the queue length is the cumulative difference between arrivals and departures; (3) says that the arrivals into queue i is the sum of exogenous arrivals and those routed to i from other queue; (4) says that queue i is served at its service rate $c_i(t)$. This is a nonlinear delay-differential inclusion. Although the inclusion is not Lipschitz, Muralidharan et al. (2015) show that the system has a unique solution for $x_i(0) \geq 0$. The 'input parameters' of the system are the rates $\{e_i(t)\}$ and the initial state $x(0)$.

The system (2)-(4) is positively homogeneous of degree one. That is, if $\{x(t),a(t),b(t)\}$ is the solution for a specified $\{x(0),e(t),c(t)\}$ and $\gamma > 0$, then $\{\gamma x(t),\gamma a(t),\gamma b(t)\}$ is the solution for $\{\gamma x(0),\gamma e(t),\gamma c(t)\}$. Hence if the exogenous arrivals e and the saturation flow rate are both increased by a factor γ, the queue $x(t)$ and the departures $b(t)$ both increase by the same factor. Thus the model predicts the first benefit of higher service rate (by platooning), namely, throughput increase.

What about queue length and delay? The average queue length at i over (say) a time interval of length τ beginning at time t_0 in the base case ($\gamma = 1$) is

$$\bar{x}_i(t_0) = \frac{1}{\tau}\int_{t_0}^{t_0+\tau} x_i(t)dt,$$

and if the service rate and arrivals (and the initial queue $x(0)$) are increased by a factor γ, the average queue length over the same time interval also increases by the same factor:

$$\frac{1}{\tau}\int_{t_0}^{t_0+\tau} \gamma x_i(t)dt = \gamma \bar{x}_i(t_0). \tag{5}$$

Since the queue length, arrival and departure processes all increase by the same factor, it is immediate that the average delay per vehicle in each queue is *unchanged*. Since the travel time is the sum of the queuing delays and the free flow travel time along a route, and both of these are unchanged by the scale factor γ, it follows that the travel time is unchanged as well.

In summary, the fluid network model yields two predictions: If the saturation flow for every movement is increased by a factor γ, then (1) the network can support a throughput that increases by γ, while (2) the queuing delay and travel time remain unchanged.

3.1 Queues with finite capacity: An example

In the queuing model above, the queue capacity is infinite. Since the queues grow in proportion to the scale factor γ of the saturation rates, the link may become saturated, and the throughput gain may be less than γ. We illustrate this in a simple example using the fluid model. Rigorous analysis of the queuing network with finite capacity queues appears to be a difficult problem.

Consider a single queue with capacity of 20 vehicles, so arrivals are blocked once the queue length reaches 20. Consider a constant arrival rate, $e(t) = a(t) = 10$, and the following service rate in one period $T = 2$:

$$c(t) = \begin{cases} 0, & t \in [0,1) \\ 30, & t \in [1,2) \end{cases}.$$

Then $\bar{c} = 15 > \bar{a} = 10$, so the queue is stable. If $x(0) = 0$, the trajectory is periodic with period T and easily calculated to be

$$x(t) = \begin{cases} 10t, & t \in [0,1) \\ \max(30-20t,0), & t \in [1,2) \end{cases}.$$

The maximum queue-length occurs at the end of red, at $t = 1 + nT$, $n = 0,1,\cdots$, and equals $x(1) = 10$.

Now suppose that the saturation flow rate and the arrival rate are increased by a factor of 3. Then $\bar{c} = 3 \times 15 = 45$ will also be the maximum throughput of the system in the case of infinite capacity, and the queue will increase by a factor of 3, so the maximum queue length will be 30. This is beyond the capacity of 20 vehicles for the finite capacity queue. If the arrival rate is $a(t) = 3 \times 10 = 30$, the queue will be blocked during the interval $t \in [2/3, 1]$. The maximum throughput of the system is easily calculated to be $\frac{20+30}{2} = 25 = 5/9 \times 45$, which is only 55 percent of the maximum throughput of the system with infinite-capacity queue.

The storage capacity of the link rather than the intersection has now become the bottleneck, so the throughput gain is reduced to a sub-linear function of the gain γ in the saturation flow rates. Note, however, that whether a link becomes a bottleneck is difficult to determine since it depends on the signal control and the offsets.

Suppose the cycle length is decreased to $T = 2/3$ and the green ratio is unchanged while the saturation flow rate is increased by 3. Then the throughput will still increase by 3, as no blocking of the queue occurs. This suggests that queues are reduced if the cycle length is reduced, while keeping the green ratios (the g_i/T) in (1) the same.

3.2 Reducing cycle time, queue length and delay

We formalize the intuition in the previous example. In the model (2)-(4) change the service rate to $c(gt)$, where $g > 1$. This means that the cycle time is reduced by g, but the green ratios are unchanged. Let $z(t) = g^{-1}x(gt)$. Then

$$\dot{z}_i(t) = \dot{x}_i(gt) = a_i(gt) - b_i(gt),$$

$$b_i(gt) = \begin{cases} c_i(gt), & \text{if } x_i(gt) > 0 \leftrightarrow z_i(t) > 0, \\ \in [0, c_i(gt)(t)], & \text{if } x_i(gt) = 0 \leftrightarrow z_i(t) = 0, \\ 0, & \text{if } x_i(gt) < 0 \leftrightarrow z_i(t) < 0. \end{cases}$$

Furthermore from (3)

$$a_i(gt) = e_i(gt) + \sum_{j=1}^{J} b_i(gt - \tau(j,i))r(j,i).$$

Hence $z(t) = g^{-1}x(gt)$ is the queue for exogenous arrivals $e(gt)$, and service $c(gt)$. Thus by speeding up the service rate by factor of g, the queue length is reduced by the same factor. This is the third prediction.

The third prediction is of a different character, since it has nothing to do with increasing saturation flow rate. However, in practice reducing cycle time is not possible because it will lead to a reduction in throughput (the constant lost time due to all-red clearance intervals is subtracted from a shorter cycle, hence the throughput is reduced), and the base case demand may not be accommodated. But if platooning gives a gain of γ in throughput, some of the gain may be used to reduce cycle time, queue length and delay.

4 Case study

We now present a simulation study of a road network near Los Angeles with 16 intersections and 73 links, using a mesoscopic simulator called PointQ. The simulator and the network are described in Tascikaraoglu et al. (2015), which reports the base case with exogenous demands at the input links, modeled as stationary Poisson streams, and intersections regulated by fixed time (FT) controls and offsets. PointQ is a discrete event simulation; it accurately models vehicle arrivals, departures and signal actuation. It models queues as 'vertical' or 'point' queues that discharge at the saturation flow rate when the signal is green, and are fed by exogenous arrivals or by vehicles that are routed from other queues. When a vehicle is discharged from one queue it travels to a randomly assigned destination queue

according to the probability distribution specified by the routing parameters $r(j,i)$ (see (3)). The vehicle takes a pre-specified fixed time to travel along the link determined by the assigned destination and then joins the destination queue. Every event in the simulation is recorded and uploaded into a database from which the reported performance measures are calculated.

Figure 3 shows a map of the study site and its representation as a directed graph with 16 signalized intersections, 73 links, and 106 turn movements, hence 106 queues. Each queue corresponds to a movement, so it is convenient to index a queue by a pair (m,n) in which m (n) is the incoming (outgoing) link index. For example, referring to Figure 3, $x(139,104)$ is the number of vehicles in link 139 that are queued up at intersection 103 waiting to go to link 104.

For the first set of experiments we increase all the saturated flow rates and the demands by the same factor $\gamma = 1.0, 1.5, 2.0, 2.5, 3.0$, with $\gamma = 1.0$ being the base case. For the second set of experiments we replace the fixed-time control by the max pressure (MP) adaptive control under two switching regimes: MP4 permits four phase changes per cycle just like for FT control, while MP6 permits six phase changes. For each experiment we present mean values of queue lengths and queuing delay. Each stochastic simulation lasts 3 hours or 10,800 sec. Since we want to calculate the mean values of queue lengths and delays, and since the queue length process is positive recurrent, it is reasonable to assume that the time average of these quantities over a three-hour long sample path will be very close to their statistical mean. Hence the mean values reported below are the empirical time averages. The results confirm all three predictions.

Queue lengths Figure 4 shows plots of the sum of all queues for three controls: FT (fixed time), MP4 (4 switches per cycle) and MP6 (6 switches per cycle) when the demand and saturation flow rates are scaled by $\gamma = 1.5$ and 3 times the base case. Notice that the queue lengths for $C = 3$ times demand are approximately twice as large than for $\gamma = 1.5$, for all three signal control schemes, as predicted by (5).

γ, Total vph	Signal Control Type	Mean Sum all queues (veh)	Ratio of sum to $C = 1$
1.0, 14350	FT	197.4	1
1.0, 14350	MP4	146.5	1
1.0, 14350	MP6	101.9	1
1.5, 21455	FT	248.6	1.26
1.5, 21455	MP4	213.7	1.49
1.5, 21455	MP6	146.8	1.46
2.0, 28540	FT	347.0	1.76
2.0, 28540	MP4	301.1	2.1
2.0, 28540	MP6	201.1	1.99
2.5, 35950	FT	455.7	2.31
2.5, 35950	MP4	395.0	2.7
2.5, 35950	MP6	248.7	2.46
3.0, 43298	FT	586.2	2.97
3.0, 43298	MP4	470.0	3.2
3.0, 43298	MP6	298.3	2.95

Table 1. Mean total queue length for different demands and signal control.

Table 1 reports the average sum of all queue lengths. The first column gives the scale factor γ and the average total exogenous demand in vph, e.g. the first column entry in the first row, (1.0, 14,350), refers to the base case $C = 1$ with an exogenous demand of 14,350 vph. The second column indicates the signal control strategy used: FT is fixed time, MP4 is max pressure with 4 changes per cycle, and MP6 is max pressure with 6 changes per cycle. The third column is the average number of vehicles summed over all 106 queues. The fourth column is the ratio of the sum of queue lengths to the sum for the base case, $\gamma = 1$. As is seen in the fourth column, this ratio is roughly equal to the scale factor, γ. For example for FT, the sum of queue lengths grows in the proportion 1: 1.26: 1.76: 2.31: 2.97 as the scale increases in the proportion 1: 1.5: 2.0: 2.5: 3.0. This is in conformity with predictions (1) and (2). First, the queue sums are staying bounded, so the increase in the saturation flows by γ does support demands that increase in the same proportion, and the queue lengths grow in the same proportion.

Queue delay We now consider queuing delay. The prediction is that the mean queuing delay experienced by a vehicle stays the same despite the increase in demand. Since there are 106 queues in all, we narrow our focus to the six queues at intersection 103. Table 2 gives the delays of each queue as a function of five values of the scale factor γ and three different signal control: FT, MP4 and MP6. Consider for example the queue $x(138,140)$. As the saturation flow rates and the demand increase in proportion 1: 1.5: 2.0: 2.5: 3.0, the mean delay (sec) in this queue under FT changes within a narrow range 22.35: 17.50: 18.99: 19.95: 20.69, while under MP4 the delay varies within the range [10.12, 11.30] and under MP6 the range is [6.73, 7.3]. When the delay is averaged over all queues at intersection 103, the variation with changes in demand is even smaller as is seen in Table 3. Note that three queues at intersection 103 correspond to right turn (RT) movements. Since right turns on red are permitted the impact of increased rates of demand and saturation flow may not be adequately captured by the three models. For this reason, Table 3 reports delays with and without including RT queues.

Faster phase switching We now come to the third prediction: queue lengths will decline as the number of phase switches per cycle increases (equivalently, the cycle time is reduced). This is borne out when we compare the sum of queue lengths for MP4 vs MP6, for each level of demand. MP4 permits four and MP6 permits 6 switches per cycle. As Table 1 shows, the queues for MP6 are indeed smaller than for MP4.

In fact the model suggests a quantitative prediction. In §3.2 g is the switching speed up, $g = 1$, being the base case. If we take MP4 as the base case, then MP6 corresponds to $g = 1.5$ (six vs four phase switches per cycle). So the mean queue length under MP4 should be 1.5 times the mean queue length under MP6, for every demand. Going back to Table 1, we see that the ratios of the sum of queue lengths under MP4 to the length under MP6 are: 1.45, 1.46, 1.5, 1.6, and 1.6 for $C = 1, 1.5, 2.0, 2.5$ and 3.0. A similar prediction is upheld in Table 3: the ratio of delays under MP4 and MP6 at queues in intersection 103 lie within a narrow band around 1.7 which can be compared to a switching speed up of $g = 1.5$.

5 Platooning challenges

If vehicles cross an intersection in platoons with a time headway of 1s, the resulting saturation flow rate will be 3,600 vps, approximately double what is seen in today's intersections. From experiments reported in the literature, such headways can be achieved by CACC. CACC is not standard in today's vehicles, but this capability is obtained by enhancing ACC with V2V communications.

γ	RT	Queue (Movement)	Delay (sec) FT	Delay (sec) MP4	Delay (sec) MP6
1.0	RT	*x*(103,104)	5.82	3.60	2.91
1.0	-	*x*(103,108)	3.07	13.60	8.94
1.0	RT	*x*(138,108)	3.76	3.48	3.28
1.0	-	*x*(138,140)	22.35	11.30	7.30
1.0	RT	*x*(139,203)	2.48	2.42	2.33
1.0	-	*x*(139,104)	21.62	11.17	7.49
1.5	RT	*x*(103,104)	4.22	3.41	2.46
1.5	-	*x*(103,108)	2.36	13.70	7.14
1.5	RT	*x*(138,108)	0.80	2.34	2.31
1.5	-	*x*(138,140)	17.50	10.71	6.76
1.5	RT	*x*(139,203)	0.73	1.57	1.56
1.5	-	*x*(139,104)	18.04	10.72	6.77
2.0	RT	*x*(103,104)	5.08	3.19	2.27
2.0	-	*x*(103,108)	2.30	14.28	6.84
2.0	RT	*x*(138,108)	0.88	1.99	1.93
2.0	-	*x*(138,140)	18.99	10.78	7.20
2.0	RT	*x*(139,203)	0.75	1.25	1.25
2.0	-	*x*(139,104)	19.1	11.09	7.16
2.5	RT	*x*(103,104)	5.67	3.48	2.28
2.5	-	*x*(103,108)	2.19	14.91	6.77
2.5	RT	*x*(138,108)	0.94	1.48	1.43
2.5	-	*x*(138,140)	19.95	10.35	6.96
2.5	RT	*x*(139,203)	0.76	1.02	1.00
2.5	-	*x*(139,104)	19.73	10.93	7.19
3.0	RT	*x*(103,104)	6.15	3.65	2.30
3.0	-	*x*(103,108)	2.09	15.79	8.06
3.0	RT	*x*(138,108)	1.08	1.08	1.07
3.0	-	*x* (138,140)	20.69	10.12	6.73
3.0	RT	*x*(139,203)	0.79	0.79	0.78
3.0	-	*x*(139,104)	20.5	10.13	6.85

Table 2. Delays in all queues at intersection 103. RT means right turn.

γ	Delay w RT FT	Delay w RT MP4	Delay w RT MP6	Delay wo RT FT	Delay wo RT MP4	Delay wo RT MP6
1.0	9.9	7.6	5.4	15.7	12.0	7.9
1.5	7.3	7.1	4.5	12.7	11.7	6.9
2.0	7.9	7.1	4.4	13.5	12.0	7.1
2.5	8.2	7.0	4.3	14.0	12.1	7.0
3	8.6	6.9	4.3	14.4	12	7.2

Table 3. Average delay at intersection 103. RT means right turn.

Milanes et al. (2014) report a cooperative adaptive cruise control (CACC) experiment involving a four-vehicle platoon with a time-headway of 0.6s at 55 mph, with cut-in and cut-out maneuvers. The vehicles came with factory-installed ACC and lidar; an additional unit with DSRC V2V communications permitted the tighter headway of 0.6s compared with the 1.1s ACC headway. The 'start' signal is easily implemented. Implementing the 'stop' signal could be left to the driver: she should not enter the intersection after end of green, like today. Indeed in CACC mode each vehicle is simply following the vehicle ahead, so the vehicles will cross an intersection as a platoon.

Platooning may require additional control logic. The platoon should start either when the first driver moves or because the start of green was signaled by the traffic controller. The platoon will terminate either because a driver stopped at a red light or disengaged from CACC mode. There are additional questions that we are unable to address. Should the intersection provide a target speed? Should it suggest a minimum or maximum platoon size? Should vehicles continue in platoon formation after crossing the intersection?

6 Conclusion

Intersections are the bottlenecks of urban roads, since their capacity is about one quarter of the maximum vehicle flow that can be accommodated by the approaches to the intersection. This bottleneck capacity can be increased by a factor of two to three if vehicles are organized to cross the intersection in platoons with 0.75s headway at 45 mph or 0.7s headway at 30 mph to achieve a saturation flow rate of 4800 vph per lane. It seems reasonable to predict that CVT can bring about a pure 'productivity increase' in the capacity of intersections of γ equal to 200 to 300 percent .

This productivity increase may be used to dramatically improve mobility. The network can support an increase in demand by the same factor γ, with no increase in queuing delay or travel time, and using the same signal control. However, the queues will also grow by the same factor γ, so if this leads to a saturation of the links, the improvement in throughput will be sub-linear in γ. On the other hand, if the cycle time is reduced by a factor g, the queues and delays will also be reduced, and this may restore the linear growth in demand.

References

T-C. Au, S. Zhang, and P. Stone. Autonomous intersection management for semi-autonomous vehicles. In *Handbook of Transportation*. Routledge, Taylor & Francis Group, 2015.

D. Bezzina and J. Sayer. Safety pilot model deployment: Test conductor team report. Report No. DOT HS 812 171, Washington, DC: National Highway Traffic Safety Administration., June 2015.

J. Harding, G.R. Powell, R. Yoon, J. Fikentscher, C. Doyle, D. Sade, M. Lukuc, M. Simons, and J. Wang. Vehicle-to-vehicle communications: Readiness of V2V technology for application. Report No. DOT HS 812 014, Washington, DC: National Highway Traffic Safety Administration., August 2014.

, R. Kianfar, B. Augusto, A. Ebadighajari,U. Hakeem, J. Nilsson,A. Raza, R. Tabar, V.N.C. Englund, P. Falcone, S. Papanastasiou,L. Svensson, and H. Wymeersch Design and experimental validation of a cooperative driving system in the grand cooperative driving challenge. *IEEE Trans. Intelligent Transportation Systems*, 13:3, 994–1007, 2012.

V. Milanes, S. E. Shladover, J. Spring, Christopher Nowakowski, H. Kawazoe, and M. Nakamura. Cooperative adaptive cruise control in real traffic situations. *IEEE Trans. Intelligent Transportation Systems*, 15(1):296–305, Feb 2014.

A. Muralidharan, R. Pedarsani, and P. Varaiya. Analysis of fixed-time control. *Transportation Research Part B: Methodological*, 73:81–90, March 2015.

J. Ploeg, B. T. M. Scheepers, E. van Nunen, N. van de Wouw, and H. Nijmeijer, Design and experimental evaluation of cooperative adaptive cruise control. *Proc. 14th ITSC IEEE Conf*, 260–265, 2011.

F. Y. Tascikaraoglu, J. Lioris, A. Muralidharan, M. Gouy, and P. Varaiya. Pointq model of an arterial network: calibration and experiments, July 2015. `http://arxiv.org/abs/1507.08082`.

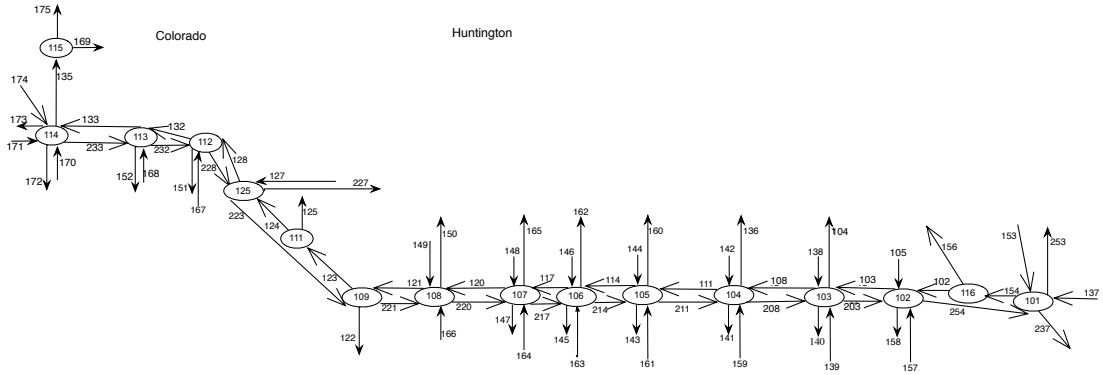

Fig. 3. Network graph of study site. The circles are intersections, links are roads.

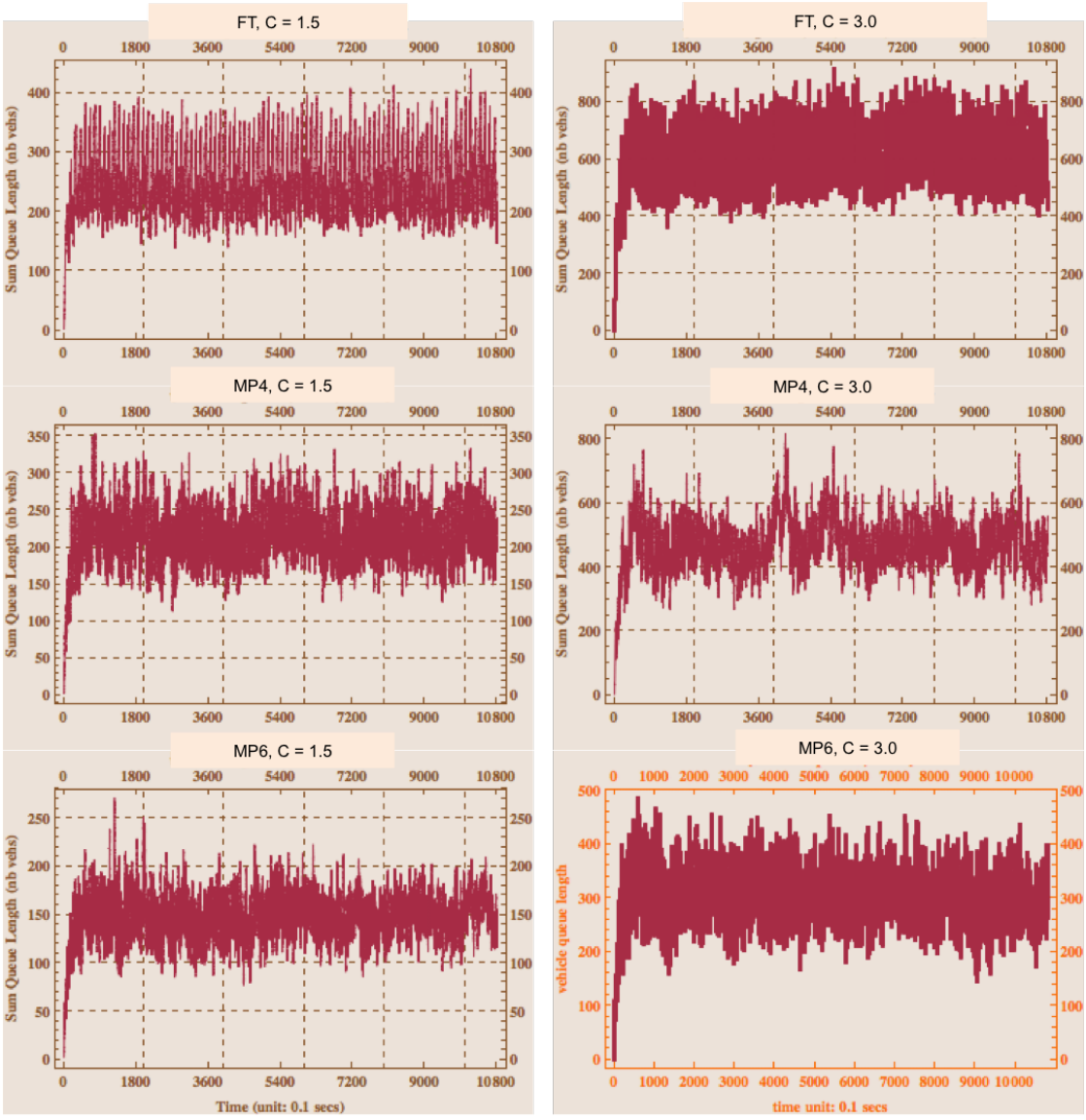

Fig. 4. Sum of all queues for FT, MP4, MP6 control when demand and saturation flows are scaled by $\gamma = 1.5$ and 3.0.